ISSN : 0974 - 7486 Volume 9 Issue 10

Trade Science Inc.

Materials Science

An Indian Journal

Full Paper

MSAIJ, 9(10), 2013 [395-401]

Analysis of the evolutions of the local mechanical properties through the carbon-enriched sub-surface of a cemented steel bar using image analysis

Patrice Berthod

Institut Jean Lamour (UMR 7198), Team 206 "Surface and Interface, Chemical Reactivity of Materials"
University of Lorraine, Faculty of Science and Technologies, B.P. 70239, 54506 Vandoeuvre-lès-Nancy, (FRANCE)
E-mail: Patrice.Berthod@univ-lorraine.fr

ABSTRACT

Some pieces made of carbon steel may be easily modified about their surface and sub-surface microstructure by carbon enrichment and inwards diffusion at high temperature, for example by applying the cementation technique. After this operation and cooling from the austenitic domain down to room temperature these pieces are usually characterized by an outer microstructure containing hard phases and compound (pro-eutectoid cementite and pearlite) while the bulk's microstructure has become the initial one (ferritic or ferritic-pearlitic) since not reached by the added carbon atoms. Thus the improved wear resistance of the outer part of the piece is not accompanied by any loss of ductility, impact toughness or resistance against cracks propagation. For a more complete knowledge of the evolution of the overall mechanical behaviour from surface to the piece's centre it is possible to use Nital etching (colouring pearlite in grey and letting bright both free cementite and ferrite) and image analysis to quantify the microstructure evolution and then the new carbon distribution. That is what was undertaken here for a cemented carbon steel bar, with in parallel a study of the evolution of mechanical properties of several carbon steels in order to get laws of variation, on the carbon content, of hardness, ultimate tensile strength and rupture strain. The combination of the two works led to specify the local values of the three above properties and then their evolution through the cemented bar under study, mechanical data which can be of importance for further mechanical modelization calculations.

KEYWORDS

Carbon steel bar;
Cementation;
Ferrite/pearlite;
Image analysis;
Mechanical properties.

INTRODUCTION

Thanks to the existence of two phase diagrams, one stable (austenite-graphite) and one metastable (austenite-cementite), as well as to a great number of different possible phases (of equilibrium or not) the iron-carbon binary system offers a very broad variety of microstructures. From ferritic steels to pearlitic steels and even hyper-eutectoid steels, from white to grey cast irons with various ferritic/pearlitic matrixes and graphite morphologies and fineness with characters varying between hypo-eutectic and hyper-eutectic, with eventually not

stable phases possible to obtain by special heat treatments (bainite, martensite...), these extremely diversified microstructures are able to bring also a very large spectrum of properties, notably in the mechanical field.

Among the mechanical properties often desired there is for example a high level of hardness, which can be achieved by the appearance of hard phases during fast solidification (ledeburite formation during eutectic solidification of white cast irons, precipitation of pro-eutectic cementite in hyper-eutectic cast iron)[1,2], fast cooling in solid state from the austenitic domain (e.g. pearlite formation in spheroid graphite cast iron)[3], or extremely fast cooling from the austenitic domain (e.g. water-quenching of steels)[4].

If a high hardness is generally intended for pieces' surface and sub-surface to resist wear for example, this is unfortunately often accompanied by a significant loss of ductility and impact toughness for the piece's bulk if the whole piece either presents an homogeneous chemical composition and similar cooling rates between its outer part and its inner part. To personalize the mechanical properties differently for these outer and inner parts a first possibility is to quickly heat up to 900 or 1000°C for example the surface of the piece (e.g. by rapid high frequency induction heating) and avoiding such increase in temperature for the bulk, then quickly cool this surface for example by water aerosol quenching, in order to obtain outer martensite and keep the initial ferritic-pearlitic structure in the bulk. Besides such surface hardening at constant chemical composition it is also possible to enrich in carbon the surface and sub-surface of the piece when heated at a temperature high enough to be austenitic, with as result a pearlitic external part and an internal part transformed again in ferritic-pearlitic as initially. Carbon cementation, technique known from a lot of decades ago[5,6], is precisely a possible route to obtain such result. Cementation of carbon is still used today for achieving such gradients of mechanical properties for steels[7,8] but cementation of other elements (chromium for example[9]) is also commonly used for achieving special mechanical properties for surfaces as well as other types of properties such as resistance against oxidation at high temperature and hot corrosion by condensed or molten aggressive substances[10-12].

The heterogeneity of mechanical properties resulting from carbon cementation may be known in some cases, for example for correctly modelizing the mechanical behaviour of the surface-hardened piece when it is subjected to stresses. For such calculations it is often required to know the local tensile strength or ductility for example, properties varying continuously from the surface to the bulk. This is exactly what was intended in the present work, about a bar made of a ferritic-pearlitic steel hardened on surface and in sub-surface by carbon cementation. For that the dependence of several mechanical properties of steel on the carbon content was preliminarily studied, before using the obtained relations to interpret in terms of mechanical behaviour the gradients of ferrite and pearlite surface fractions measured by image analysis.

EXPERIMENTAL DETAILS

The cemented steel bar of interest

The steel bar enriched in carbon by cementation when it was stabilized in its austenitic state (i.e. near 1000°C) had a diameter of about 10mm. It is represented in Figure 1 by a scheme and a macrograph taken after the confection of a mounted sample (cutting, embedding in a cold resin mixture, polishing with grinding papers with grades from 120 to 1200, ultrasonic cleaning, final polishing with textile enriched with 1µm hard particles, 10 seconds etching in Nital4: 96vol.% ethanol + 4vol.% HNO_3). The grey outer part of the bar is due to a microstructure which is almost wholly of lamellar pearlite (and in the extreme surface even pearlite + pro-eutectoid cementite formed during post-cementation cooling in the old grain boundaries of the austenite existing at high temperature), while the central main part of the bar is significantly brighter, this showing that the initial ferrite-pearlite was recovered after return to room temperature. The fact that the microstructure gradually varies from an hyper-eutectoid form in extreme surface to a ferritic-pearlitic form several millimeters deeper means that the local mechanical properties themselves evaluate over the same distance.

Quantification of the microstructure {extreme surface → bar center}and of the carbon distribution

Successive micrographs were taken using the numeric camera equipping an optical microscope on the

etched sample from the external surface and at an increasing depth along a line perpendicular to the edge (step: every 250µm). These micrographs were analyzed by using the surface fraction quantification tool of the Photoshop CS software to assess at each depth the surface fraction of pro-eutectic cementite, of pearlite and of ferrite. Assuming thereafter that these surface fractions can be considered as volume fractions, and furthermore as mass fractions since the volume mass or density is sensibly the same for ferrite and cementite and thus of pearlite which is a compound mixing the two later phases, i.e. about 7.8g cm^{-3}, it appears possible to determine the local carbon content by: %C ≈ {pro-eutectoid cementite fraction} × 6.67wt.%C + {pearlite fraction} × 0.77wt.%C + {ferrite fraction} × 0wt.%C. It becomes thereafter thus possible to deduce from the image analysis results the repartition of mass content in carbon perpendicularly to the extreme surface.

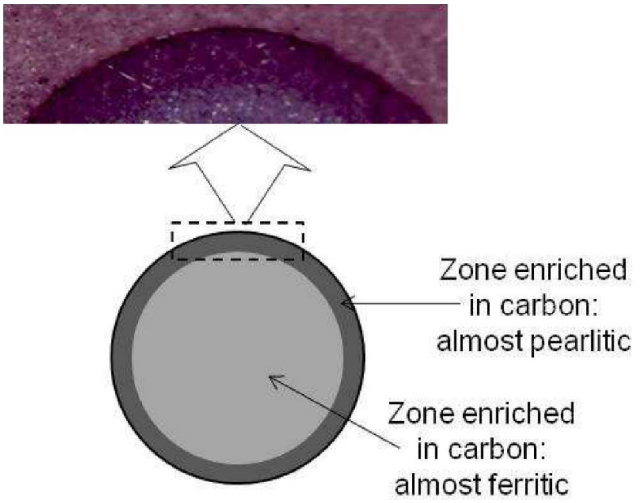

Figure 1 : Scheme of the cemented steel bar and local macrograph showing the structure gradient from the external surface (after Nital4 etching).

Mechanical tests performed on several varieties of carbon steels

Six different carbon steels were selected in another study to cover the microstructure range observed through the bar described above. These steels were a ferritic one, three ferrite-pearlite ones with an increasing {pearlite / ferrite}-ratio, a pearlitic one (fully eutectoid) and a hyper-eutectoid one, with in all cases (except the ferritic steel) a lamellar fineness of pearlite similar to the pearlite observed in the cemented bar. Vickers indentations were performed on each of them (hardness) as well as tensile tests in order to specify their ultimate tensile strength (resistance in traction) and rupture elongation (ductility).

By plotting the four mechanical properties versus the steel carbon content it becomes possible to deduce laws of dependence of these properties on the carbon content, before using them to translate the carbon content evolution across the cemented bar in properties' evolutions.

RESULTS AND DISCUSSION

Inward microstructure evolution from the surface of the cemented bar

The inward microstructure evolution is illustrated by the micrographs taken every 250µm from surface in Figure 2 then in Figure 3. One can see that the microstructure in extreme surface is of the hypereutectic type since pro-eutectic cementite is present together with pearlite which is the main compound. This reveals a local carbon content slightly higher than the 0.77wt.% of pearlite. A little deeper (depth > 0.75mm) this free cementite disappears and pearlite becomes the single compound present, before ferrite begins to appear (depth > 1mm). When the observation depth goes on

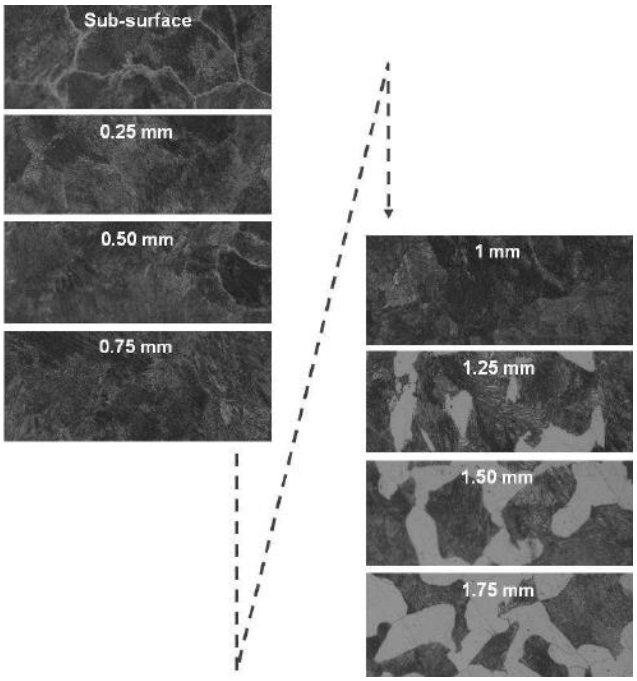

Figure 2 : Microstructure evolution over the two first millimeters from the bar surface.

increasing ferrite becomes more and more present, with the inverse evolution for pearlite. Finally, in areas deep enough, ferrite becomes again the main phase present in the bar, as it was the case before the cementation treatment.

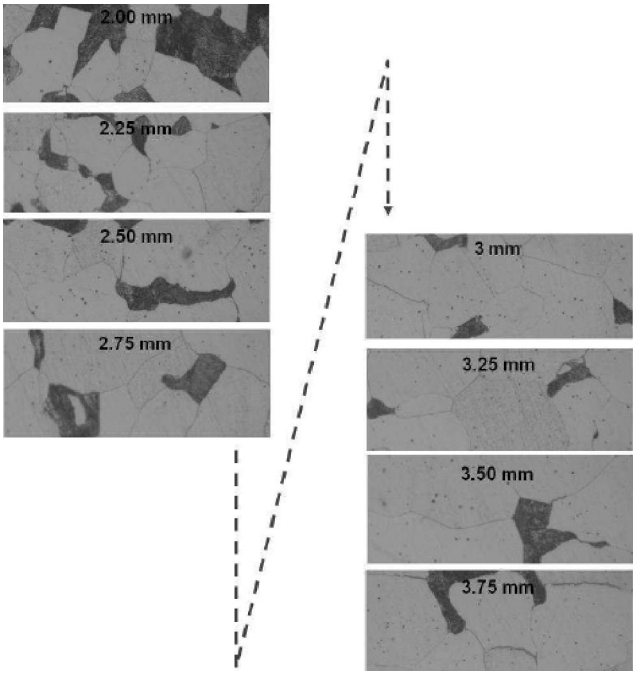

Figure 3 : Microstructure evolution over the following two millimeters from the bar surface.

By applying image analysis to these successive micrographs and thereafter the formula given above one obtains first the graph displayed in Figure 4 showing quantitatively the evolution of the surface fractions of pro-eutectic cementite (called "free cementite" by opposition to the lamellar cementite mixed with ferrite in the pearlite), of pearlite and of ferrite, and second the graph presented in Figure 5 plotting the evolution of the carbon mass content with the depth.

According to the image analysis results the surface fractions of free cementite decreases from 1.5% on the extreme surface down to 0 at 750µm and deeper. Pearlite begins to slightly increase from 98.5% on the extreme surface up to 100% at 750µm – thanks to the previously described decrease in free cementite – then starts decreasing because of the appearance of ferrite. Thus the pearlite fraction decreases from 100% at a depth of 750µm down to around 10% (the dispersion of the image analysis results does not allow to be more accurate) while at the same time ferrite which appears at 750µm increases in surface fraction upto about 90% at a depth of about 3mm and deeper. The corresponding carbon content, estimated according to the formula presented above, is at its maximum on extreme surface – 0.86% as is to say a composition slightly hyper-eutectoid conform to the hyper-eutectoid type of the local microstructure – and it decreases more or less regularly down to 0.05–0.06wt.%, value at which it becomes stabilized.

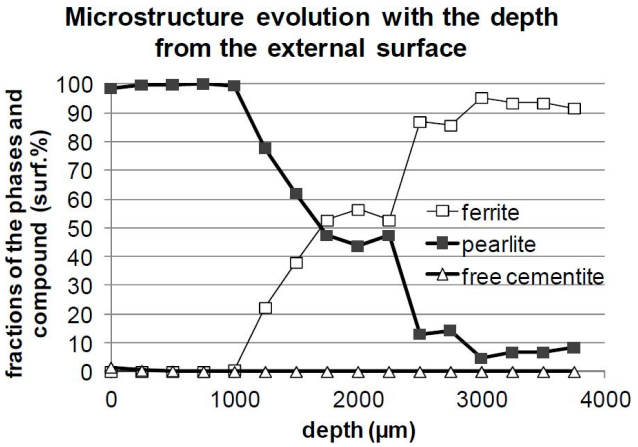

Figure 4 : Results of image analysis of pro-eutectic cementite, pearlite and ferrite plotted versus the depth counted from the extreme surface.

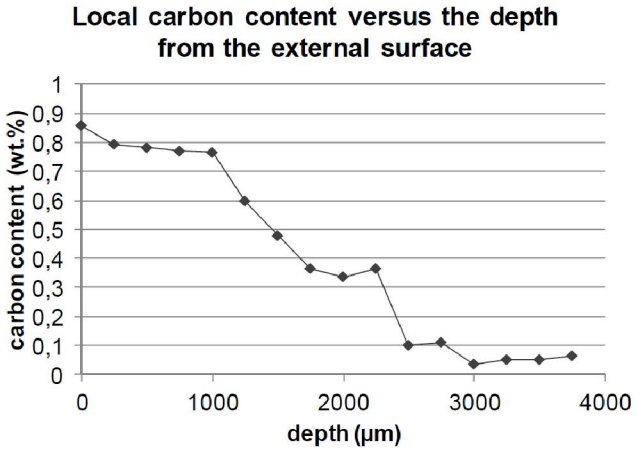

Figure 5 : The distribution of carbon (contents issued from the image analysis results) plotted versus the depth counted from the extreme surface.

Establishment of the variation laws followed by the mechanical properties versus the carbon content

Knowing now the quantitative evolutions of both the microstructure and the carbon content it appears possible to deduce the evolution of the different mechanical properties evocated above. Before that, it is necessary to exploit the corresponding test results ob-

tained for the six carbon steels with various microstructures between the pure ferritic one and the hyper-eutectoid one. The evolution of the hardness versus the carbon content is plotted in Figure 6, the one of the ultimate tensile strength in Figure 7 and the one of the strain at rupture in Figure 8.

From the ferritic steel (0wt.%C) to the hyper-eutectoid one (1.2wt.%C) the Vickers hardness increases from 80 to 220, while at the same time the ultimate tensile strength also increases from 280MPa to 750MPa and the rupture strain decreases from 50 down to 10%. These three evolutions are rather regular and it was possible for each of these three graphs to determine a polynomial law modelizing the dependence of these three mechanical properties on the carbon content of the steels. These three polynomial functions are directly given in the corresponding graphs.

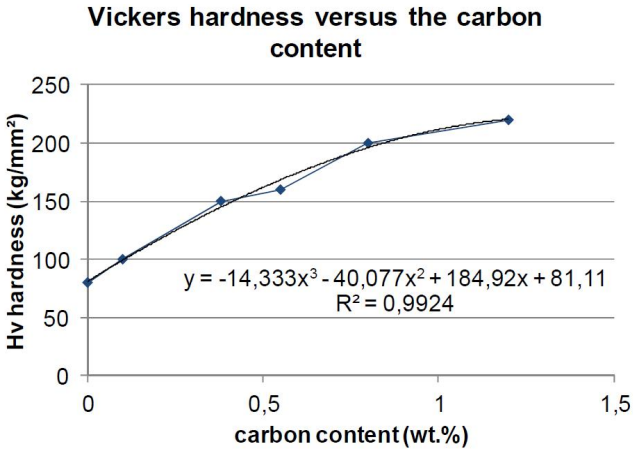

Figure 6 : Evolution of the hardness of the carbon steels versus their carbon weight contents.

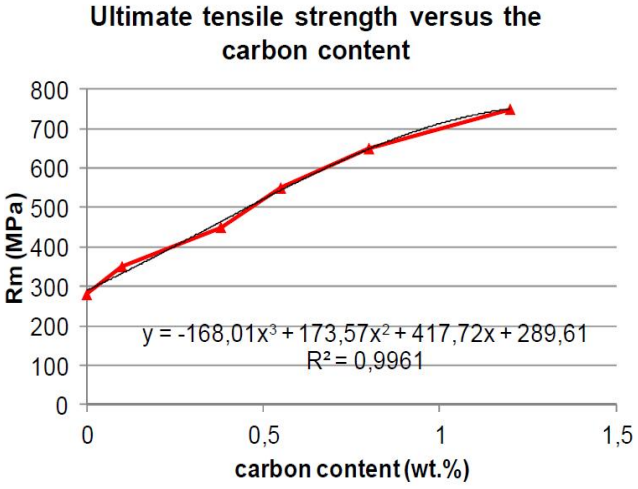

Figure 7 : Evolution of the ultimate tensile strength of the carbon steels versus their carbon weight contents.

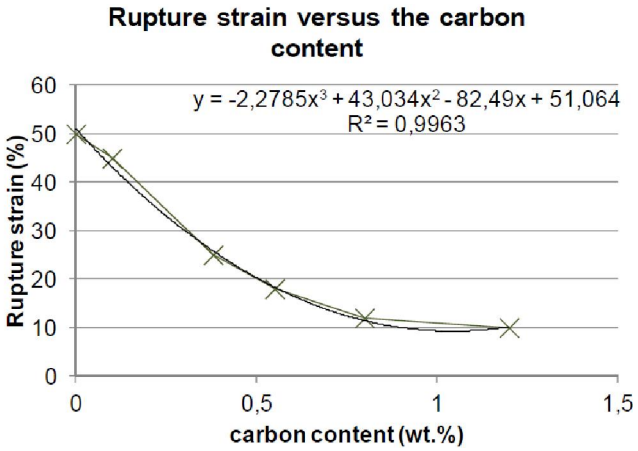

Figure 8 : Evolution of the strain at rupture of the carbon steels versus their carbon weight contents.

Evolution of the local mechanical properties with depth across the cemented sub-surface of the bar

The three polynomial laws were thereafter used to deduce, from the new carbon content distribution in the sub-surface of the cemented bar, the evolutions of the hardness, the ultimate tensile strength and the rupture strain from the extreme surface of the bar to the zone not enriched in carbon during cementation. The calculated Vickers hardness (Figure 9) decreases from 201 down to about 90 from the extreme surface (of the hyper-eutectoid type) to the ferritic-pearlitic bar core with unchanged microstructure (by comparison with before cementation). The calculated ultimate tensile strength (Figure 10) and the rupture strain (Figure 11) also vary from the outer part of the bar to its inner part: the UTS decreases from 670 to 317MPa while the ductility increases from 10.5% at 46%.

General commentaries

Carbon enrichment of steels by cementation, one of the oldest chemical vapor deposition (CVD) techniques allowing such surface and sub-surface microstructure modification by chemical composition change, promotes the formation of hard phases in the outer part of pieces for improving their wear resistance for example, without threatening the ductility and impact toughness of the bulk. In the present study image analysis allowed quantifying first the surface fractions (then volume and even mass thanks to the common value of density for the three phases and compound present) of pro-eutectoid cementite, pearlite and ferrite, and second the distribution of carbon in the carbon-enriched

outer zone. Even if the dispersion of the image analysis results did not lead to regular evolution with depth the evolution of carbon content from the extreme surface is rather representative of the inwards high temperature diffusion through the austenitic bar of carbon atoms deposited on surface by the vector gas decomposition during the cementation process. Thanks to the parallel exploitation of the dependence of several mechanical properties on the carbon content of several carbon steels, which led to approximate polynomial laws, it has been possible to translate the carbon on evolution versus depth into evolution of hardness, UTS and rupture strain (e.g. ductility). This allowed here to better know the local values of these properties and to value the thicknesses of the hard zones, the more stress-resistant zones, as well as the proportion in the bar's bulk of the part remained still ductile and tough enough to resist eventual cracks propagation.

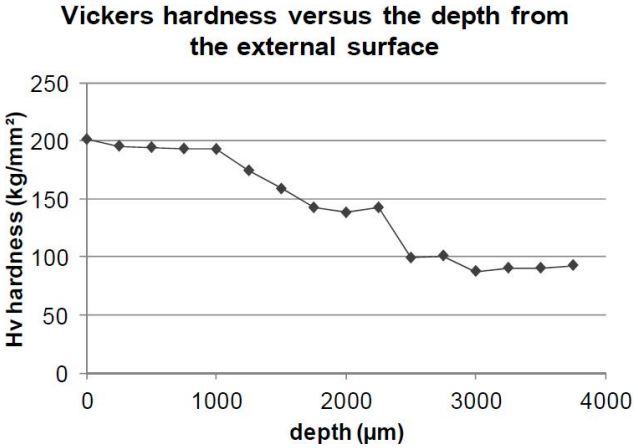

Figure 9 : Evolution of the local hardness in the bar versus the depth from the extreme surface.

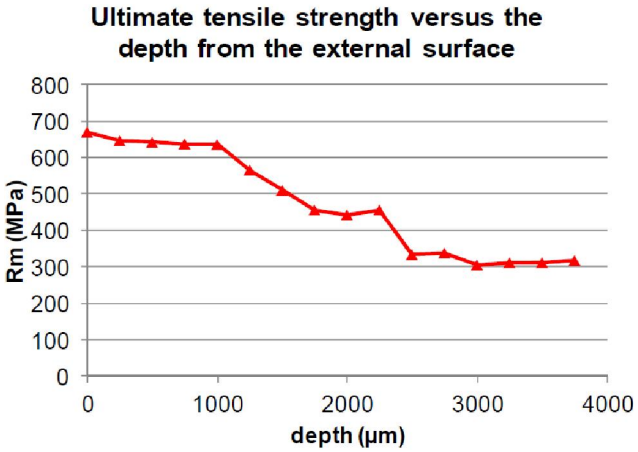

Figure 10 : Evolution of the local ultimate tensile strength in the bar versus the depth from the extreme surface.

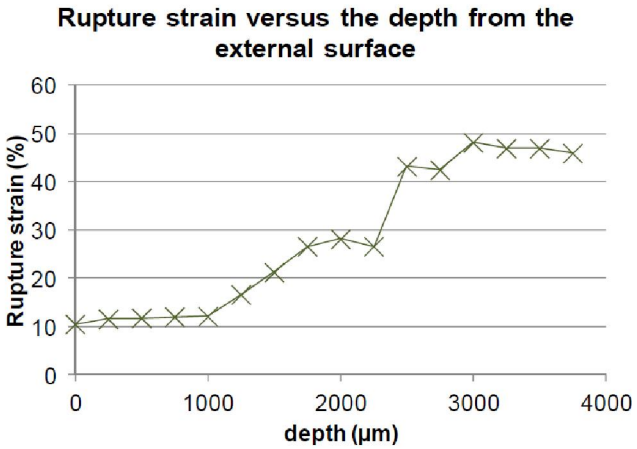

Figure 11 : Evolution of the local rupture strain in the bar versus the depth from the extreme surface.

CONCLUSIONS

Thanks to the simple dependence of the pearlite/ferrite ratio on the local carbon content, image analysis associated to the results of Nital etching on carbon steels, allows retrieving the carbon evolution trough the depth of a cemented piece, and deducing the local values of some mechanical properties. Such data may be useful for any mechanical or thermomechanical modelization calculations (in a cylindrical symmetry in the case of the studied bar), but the method {image analysis → carbon content evolution → properties evolution} may be applied to much more complex pieces made of carbon steel also enriched in carbon by cementation.

REFERENCES

[1] G.Lesoult; Solidification: Cristallisation et microstructures, Techniques de l'Ingénieur, M58, Paris, **(1986)**.
[2] W.Kurz, D.J.Fisher; Fundamentals of solidification, Trans.Tech.Publ., Switzerland, **(1989)**.
[3] M.Durand-Charre; Microstructure of steels & cast irons (Engineering materials & processes), Springer, **(2004)**.
[4] A.Litwinchick, F.X.Kayser, H.H.Baker, A.Henkin; J.Mater.Sci., **11**, 1200 **(1976)**.
[5] F.Giolitti; The cementation of iron and steel, MacGraw-Hill Book Company, London, **(1915)**.
[6] E.G.Mahin, R.C.Spencer, C.R.Hayner; Proc.Ind.Acad.Sci., **34**, 1924 **(1925)**.
[7] M.Erdogan, S.Tekeli; Materials Characterization,

49, 445 **(2003)**.

[8] L.S.Malinov, V.A.Kharhashkin; Metal Science & Heat Treatment, **3(2)**, 58 **(2011)**.

[9] J.W.Lee, J.G.Duh; Surface and Coatings Technology, **177–178**, 525 **(2004)**.

[10] G.Michel, P.Berthod, M.Vilasi, S.Mathieu, P.Steinmetz; Surface and Coatings Technology, **205**, 3708 **(2011)**.

[11] G.Michel, P.Berthod, M.Vilasi, S.Mathieu, P.Steinmetz; Surface and Coatings Technology, **205**, 5241 **(2011)**.

[12] G.Michel, P.Berthod, S.Mathieu, M.Vilasi, P.Steinmetz; The Open Corrosion Journal, **4**, 27 **(2011)**.